Spin Relaxation near the Metal-Insulator Transition: Dominance of the Dresselhaus Spin-Orbit Coupling

Guido A. Intronati,[1,2,3] Pablo I. Tamborenea,[1,2] Dietmar Weinmann,[2] and Rodolfo A. Jalabert[2]

[1]*Departamento de Física, FCEN, Universidad de Buenos Aires, Ciudad Universitaria, Pab. I, C1428EHA Buenos Aires, Argentina*

[2]*Institut de Physique et Chimie des Matériaux de Strasbourg, UMR 7504, CNRS-UdS, 23 rue du Loess, B.P. 43, 67034 Strasbourg Cedex 2, France*

[3]*Service de Physique de l'État Condensé, CNRS URA 2464, CEA Saclay, 91191 Gif-sur-Yvette, France*

(Received 21 February 2011; published 3 January 2012)

We identify the Dresselhaus spin-orbit coupling as the source of the dominant spin-relaxation mechanism in the impurity band of a wide class of *n*-doped zinc blende semiconductors. The Dresselhaus hopping terms are derived and incorporated into a tight-binding model of impurity sites, and they are shown to unexpectedly dominate the spin relaxation, leading to spin-relaxation times in good agreement with experimental values. This conclusion is drawn from two complementary approaches: an analytical diffusive-evolution calculation and a numerical finite-size scaling study of the spin-relaxation time.

DOI: 10.1103/PhysRevLett.108.016601 PACS numbers: 72.25.Rb, 03.67.−a, 72.20.Ee, 76.30.Pk

Spin dynamics in semiconductors is a fundamental issue in view of the rich physics involved and the potential technological applications [1,2]. It is thus not surprising that spin-relaxation studies were already performed in the early days of semiconductor research [3–5] and are intensely pursued today with modern experimental techniques [6,7]. An intriguing experimental observation is the fact that in *n*-doped semiconductors at low temperatures the spin-relaxation time τ_s presents a maximum as a function of the doping density near the metal-insulator transition (MIT) [5,6,8–12].

Interestingly, while the mechanisms behind spin relaxation have been properly identified at high temperatures or for doping densities away from the critical one [10,13,14], a theoretical understanding of low-temperature spin relaxation close to the MIT is still lacking. This unsatisfactory state of affairs has motivated some attempts to identify the relevant mechanisms for spin relaxation [15–19] in this regime. In particular, on the metallic side of the transition, Shklovskii proposed the applicability of the well-known Dyakonov-Perel mechanism usually valid in the conduction band [15]. Furthermore, a tight-binding model of impurities including spin-orbit coupling due to the electrostatic impurity potentials has been developed [19]. The spin-relaxation times resulting from this last model are larger than the experimental values, implying that other mechanisms should be active in this density regime.

In this work we identify the Dresselhaus coupling as the source of the leading spin-relaxation mechanism on the metallic side of the transition for zinc blende semiconductors. This conclusion is based on the construction of an effective spin-orbit Hamiltonian for the impurity system, together with its analytical and numerical solution. The resulting spin-relaxation times are in good agreement with the existing experimental values for GaAs and CdTe. The detailed temperature-dependent measurements of Ref. [11] yielded a saturation of τ_s below 10 K, indicating that inelastic processes are irrelevant at low temperatures. We thus work with a zero-temperature formalism.

The envelope-function approximation for describing conduction-band electrons in zinc blende semiconductors incorporates the lattice-scale physics (described by the periodic part of the Bloch wave function) into the effective one-body Hamiltonian [20,21]

$$H = H_0 + H_{\text{extr}} + H_D, \tag{1}$$

$$H_0 = \frac{p^2}{2m^*} + V(\mathbf{r}), \tag{2}$$

$$H_{\text{extr}} = \lambda \boldsymbol{\sigma} \cdot \nabla V \times \mathbf{k}, \tag{3}$$

$$H_D = \gamma[\sigma_x k_x (k_y^2 - k_z^2) + \text{cyclic permutations}]. \tag{4}$$

Here $\boldsymbol{\sigma}$ is the vector of Pauli matrices and $\mathbf{k} = \mathbf{p}/\hbar$. The extrinsic term stems from $V(\mathbf{r})$, which includes all potentials aside from the crystal one. The effective spin-orbit coupling λ is usually orders of magnitude larger than the one of vacuum $\lambda_0 = \hbar^2/4m_0^2c^2 \simeq 3.7 \times 10^{-6}$ Å^2. It can be calculated at the level of the 8-band Kane model, which, for example, for GaAs yields $\lambda \simeq -5.3$ Å^2 [21]. The Dresselhaus or intrinsic term is enabled by the bulk inversion asymmetry and depends on the material-dependent coupling constant γ. The exact value of γ for GaAs is a matter of current debate [1,21]. A 14-band model is required for the theoretical estimation of γ, leading to $\gamma \approx 27$ eV Å^3 [22]. More refined theoretical calculations yield somewhat lower values [23–25]. While early experimental values obtained in bulk samples agree approximately with the above-quoted value of 27 eV Å^3 [26],

recent results inferred from measurements in low-dimensional systems are again consistently lower [1,27–29].

In order to study the spin relaxation in the impurity band near the MIT, we consider the potential $V(\mathbf{r})$ due to the ionized impurities, given by

$$V(\mathbf{r}) = \sum_p V_p(\mathbf{r}) = -\sum_p \frac{e^2}{\epsilon|\mathbf{r} - \mathbf{R}_p|}, \tag{5}$$

where ϵ is the dielectric constant of the semiconductor and $\mathbf{R}_p$ represents the impurity positions. The potential V_p gives rise to hydrogenic states centered at the impurity p. In order to build the basis of electronic states, we will consider only the ground state $\phi_p(\mathbf{r}) = \phi(|\mathbf{r} - \mathbf{R}_p|)$, with $\phi(\mathbf{r}) = (1/\sqrt{\pi a^3})\exp(-r/a)$ and a the effective Bohr radius.

The second-quantized form of the Hamiltonian (1), that we denote $\mathcal{H}$, has components

$$\mathcal{H}_0 = \sum_{m \neq m', \sigma} \langle m'\sigma|H_0|m\sigma\rangle c^\dagger_{m'\sigma} c_{m\sigma}, \tag{6}$$

$$\mathcal{H}_{\mathrm{SO}} = \sum_{m \neq m', \sigma} \langle m'\bar{\sigma}|H_{\mathrm{SO}}|m\sigma\rangle c^\dagger_{m'\bar{\sigma}} c_{m\sigma}, \tag{7}$$

where the label SO stands for "extr" or "D." We denote the $1s$ state $\phi_m(\mathbf{r})$ with spin $\sigma = \pm 1$ in the z direction by $|m\sigma\rangle$, and $c^\dagger_{m\sigma}$ ($c_{m\sigma}$) is the creation (annihilation) operator of a particle in that state ($\bar{\sigma} = -\sigma$). The matrix elements in Eq. (6) contain three-center integrals $\langle m'\sigma|V_p|m\sigma\rangle$ with $p \neq m$. Because of the exponential decay of $\phi_m(\mathbf{r})$, one usually keeps only the term

$$\langle m'\sigma|V_{m'}|m\sigma\rangle = -V_0\left(1 + \frac{R}{a}\right)e^{-R/a}, \tag{8}$$

with $V_0 = e^2/\varepsilon a$ (twice the binding energy of an isolated impurity) and $R = |\mathbf{R}_{m'm}|$ the distance between the two impurities. The resulting Hamiltonian $\mathcal{H}_0$ defines the well-known Matsubara-Toyozawa (MT) model [30]. The subtleties, drawbacks, and applicability of this model to describe the metallic side of the MIT, as well as its extension to include the $\mathcal{H}_{\mathrm{extr}}$ spin-orbit coupling, have recently been discussed [31]. Electron-electron interactions induce significant many-body effects on the insulating side of the transition but not on the metallic side. Therefore, we do not include them in our model. According to the Mott criterion, the critical dimensionless impurity density for the MIT corresponds to $\mathcal{N}_i = n_i a^3 \simeq 0.017$, leading to a critical density of 2×10^{16} cm^{-3} for GaAs.

The matrix element of $\mathcal{H}_{\mathrm{extr}}$ is

$$\begin{aligned}\langle m'\bar{\sigma}|H_{\mathrm{extr}}|m\sigma\rangle = \frac{\sigma\lambda}{a^2}\int d\mathbf{r} V(\mathbf{r}) \frac{\phi_{m'}(\mathbf{r})\phi_m(\mathbf{r})}{|\mathbf{r} - \mathbf{R}_{m'}||\mathbf{r} - \mathbf{R}_m|} \\ \times [(z - z_m)(r_\sigma - R_{m'\sigma}) - (z - z_{m'}) \\ \times (r_\sigma - R_{m\sigma})],\end{aligned} \tag{9}$$

where $r_\sigma = x + i\sigma y$ and $R_{m\sigma} = X_m + i\sigma Y_m$. The Hamiltonian $\mathcal{H}_{\mathrm{extr}}$ takes into account the electric field arising from the impurity potentials and was introduced in Ref. [19]. There, an alternative path to the envelope-function approximation was followed in order to calculate the matrix elements $\langle m'\bar{\sigma}|H_{\mathrm{extr}}|m\sigma\rangle$, which made use of impurity states with spin admixture obtained from spin-admixed conduction-band Bloch states derived at the level of the 8-band Kane model. We remark that the terms corresponding to $p = m, m'$ in $V(\mathbf{r})$ give vanishing contributions to the matrix element (9) due to the axial symmetry of the two-center integrals. Therefore, these matrix elements are given by three-center integrals, resulting in very slow spin relaxation [19] in comparison with experimental results. We thus turn to the Dresselhaus term, whose matrix element is given by

$$\langle m'\bar{\sigma}|H_D|m\sigma\rangle = \frac{\gamma}{\pi a^3}(\sigma I_{y,m'm} + iI_{x,m'm}), \tag{10}$$

where

$$I_{x,m'm} = \frac{1}{a^3}\int d\mathbf{r} \frac{e^{-|\mathbf{r} - \mathbf{R}_{m'm}|/a} e^{-r/a}}{|\mathbf{r} - \mathbf{R}_{m'm}| r^3}(a + r)(x - X_{m'm})(y^2 - z^2) \tag{11}$$

and $I_{y,m'm}$ is obtained from $I_{x,m'm}$ with the exchanges $X_{m'm} \leftrightarrow Y_{m'm}$ and $x \leftrightarrow y$. Performing a rotation of the coordinate system and with the help of prolate spheroidal coordinates, we obtain for the previous two-center integral the remarkably simple expression

$$I_{x,m'm} = \frac{\pi c}{6}\left(\frac{R}{a}\right)^2 e^{-R/a}, \tag{12}$$

where $c = 2\cos\varphi\sin\theta[1 - \sin^2\theta(1 + \sin^2\varphi)]$ and (R, θ, φ) are the polar coordinates of $\mathbf{R}_{m'm}$ in the original reference frame.

The spatial diffusion of electrons through the network of impurities is accompanied by a small spin rotation angle at each hop. Thus, the evolution of the electron spin can be seen as diffusion on a sphere. The typical hopping time τ_c can be taken as the time needed for the initial-state population on an impurity site to drop from 1 to 1/2, that is,

$$\frac{1}{\tau_c} = \frac{\sqrt{2}}{\hbar}\left(\sum_{m \neq m'} |\langle m'\sigma|H_0|m\sigma\rangle|^2\right)^{1/2} \simeq \frac{\sqrt{14\pi}V_0}{\hbar}\mathcal{N}_i^{1/2}. \tag{13}$$

For the second equality [32], we have used the impurity average assuming a random distribution without hard-core repulsive effects on the scale of the effective Bohr radius

[19,33]. For an electron hopping between the impurities m and m', a spin initially oriented along the unit vector defined by the polar (ξ) and azimuthal (ζ) angles rotates by [19]

$$\alpha = 2\sqrt{1 + \sin^2\xi\cos^2\zeta}\,\frac{|\langle m'\bar{\sigma}|H_D|m\sigma\rangle|}{|\langle m'\sigma|H_0|m\sigma\rangle|}. \quad (14)$$

Averaging over ξ, ζ, and the impurity configurations, we can extract the mean-squared rotation angle per hop defining the spin diffusion:

$$\langle\alpha^2\rangle = \frac{16}{3}\frac{\sum_{m\neq m'}|\langle m'\bar{\sigma}|H_D|m\sigma\rangle|^2}{\sum_{m\neq m'}|\langle m'\sigma|H_0|m\sigma\rangle|^2} \simeq 0.145\left(\frac{\gamma}{a^3V_0}\right)^2. \quad (15)$$

From an initial distribution of absolute certainty that the point is at the north pole, the resulting distribution after diffusing on a sphere for a time t is given by [34]

$$\rho(\theta,t) = \sum_{n=0}^{\infty}\frac{2n+1}{4\pi}\exp\left[-\frac{1}{4}n(n+1)U(t)\right]P_n(\cos\theta), \quad (16)$$

where P_n are the Legendre polynomials and $U(t) = (t/\tau_c)\langle\alpha^2\rangle$ is the variance of the corresponding plane motion. The z component of the spin expectation value is given by

$$\langle S_z(t)\rangle = \int d\Omega\,\cos\theta\rho(\theta,t) = \exp\left[-\frac{1}{2}\frac{\langle\alpha^2\rangle t}{\tau_c}\right]. \quad (17)$$

We then have a spin-relaxation rate

$$\frac{1}{\tau_s} = \frac{1}{2}\frac{\langle\alpha^2\rangle}{\tau_c} \simeq 0.48\frac{\gamma^2}{a^6V_0\hbar}\mathcal{N}_i^{1/2}. \quad (18)$$

We remark that this expression for the spin-relaxation time is valid for all n-doped zinc blende semiconductors. The comparison with other relaxation mechanisms lets us conclude that the Dresselhaus coupling dominates in the impurity band for all zinc blende semiconductors except the narrow-gap ones.

Numerical calculations of the spin-relaxation time within our model provide an alternative path which is free of the simplifications used in the analytical approach. The numerical procedure starts with the calculation of the matrix elements (10) for H_D (and similarly for $H_{\rm extr}$) for a given impurity configuration. We then diagonalize the total Hamiltonian $\mathcal{H}$ including the two contributions to the spin-orbit coupling, which allows us to obtain the quantum evolution of an arbitrary state. Choosing an initial state with a well-defined spin projection (for instance, a MT eigenstate with $\sigma = 1$), we can follow the spin evolution and extract the spin lifetime from it. The weakness of the spin-orbit coupling translates into spin-admixture perturbation energies which are, even for the largest system sizes (in terms of the number of impurities N) that we are able to treat numerically, orders of magnitude smaller than the typical MT level spacing. This large difference between the two energy scales in finite-size simulations masks the spin-orbit-driven physics and forces us to follow an indirect path: We introduce an artificially enhanced coupling constant $\eta\gamma$ and a finite-size scaling procedure. The limits $N \to \infty$ and then $\eta \to 1$ taken at the end of the calculation provide, after impurity average, the sought spin-relaxation rate.

We now apply the numerical procedure just described to the widely studied case of GaAs. The numerically extracted values of the spin-relaxation times associated with $H_{\rm extr}$ are, consistently with the results of Ref. [19], considerably larger than the ones experimentally observed. Therefore, we hereafter neglect this term in the numerical calculations and concentrate on the spin evolution governed by H_D. In the lower inset in Fig. 1, we show typical spin evolutions starting from an eigenstate of the MT system with $\sigma = 1$ in the energy range of extended states of the impurity band, for a density $\mathcal{N}_i = 0.029$ just above the MIT transition for three values of the coupling constant and $N = 3375$ impurities. The initial perturbative regime with a quadratic time decay of the spin survival is followed by an exponential decay from which the relaxation rate τ_s^{-1} can be inferred, until the saturation value of $1/2$. For each density and effective coupling constant $\eta\gamma$, the asymptotic value of τ_s^{-1} can be obtained by extrapolating the finite-N values to the infinite-size limit (upper inset in Fig. 1). We

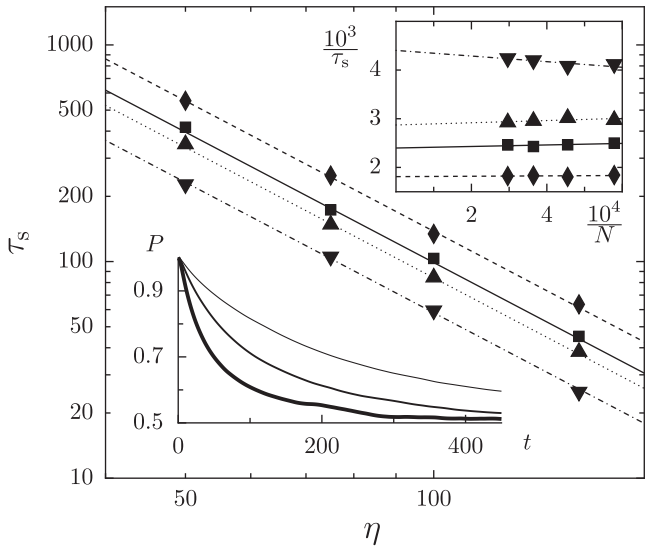

FIG. 1. Scaling of the spin-relaxation time extrapolated to infinite system size with the spin-orbit enhancement factor η, for densities $\mathcal{N}_i = 0.02$ (◆), 0.029 (■), 0.037 (▲), and 0.06 (▼). The lines are fits of a quadratic dependence of the relaxation rate on η. Times are given in units of $\hbar/V_0$. Lower inset: Spin survival probability P for an initial MT eigenstate at density $\mathcal{N}_i = 0.029$ and system size $N = 3375$. Lines of increasing thickness are for $\eta = 75$, 100, and 150. Upper inset: Size dependence of τ_s^{-1} for $\eta = 50$ at the densities of the main figure. Lines are linear fits to the data that allow us to extrapolate to the infinite-size values.

ran a sufficiently large number of impurity configurations (typically 200) to make the statistical errors negligible (smaller than the symbol size in the figure). In agreement with our analytical results, an inverse quadratic dependence of τ_s on the coupling strength is obtained (Fig. 1). Fitting this dependence of τ_s on η allows us to extract the physical values ($\eta = 1$) of τ_s.

In Fig. 2, we present the spin-relaxation times resulting from our numerical approach for GaAs at four different impurity densities above the MIT (●), together with the prediction of Eq. (18) (solid line), and the available experimental data from Refs. [6,7,10,11] (blue online). Both approaches describe the data within the experimental uncertainty and correctly reproduce the density dependence of the spin-relaxation time. The departure of the analytical and numerical results is not significant, taking into account the different approximations of both paths and the arbitrariness associated with the definition of relaxation times.

While in the critical region and deep into the localized regime there is some dispersion of the experimental values for GaAs, depending on the different samples and measurement technique, on the metallic side of the MIT values of $\tau_s \gtrsim 100$ ns are consistently obtained. A decrease of τ_s with $n_i^{1/2}$ is observed, with a clear change in the density dependence once the impurity and the conduction bands hybridize. Our analytical and numerical results of Fig. 2 (solid line and filled circles, respectively) are obtained by

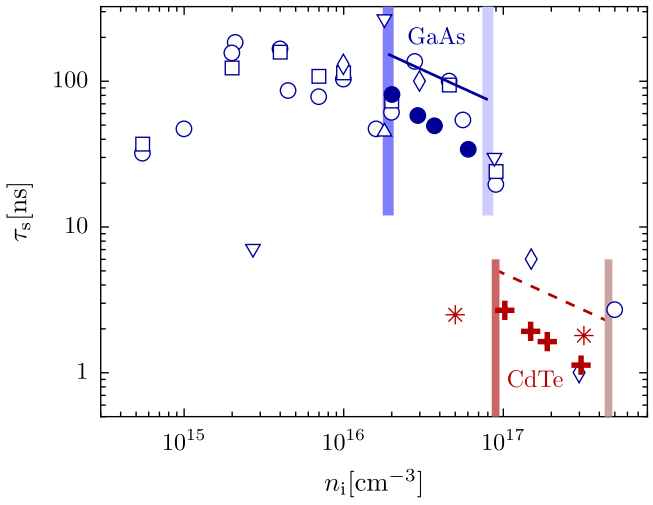

FIG. 2 (color online). Spin-relaxation time as a function of doping density. For n-doped GaAs (blue online), the prediction of Eq. (18) (solid line) and our numerical results (●) for the metallic regime between the metal-insulator transition (dark thick vertical line) and the hybridization of the impurity band with the conduction band (light thick vertical line) obtained by using $\gamma = 27$ eV Å^3 are compared to experiments. Data are taken from Ref. [10] for $T = 2$ K (○) and $T = 4.2$ K (□), Ref. [6] (◇), Ref. [7] (△), and Ref. [11] (▽). The case of CdTe (red online) is shown by the dashed line [Eq. (18)], numerical results (+), and experimental data from Ref. [12] (*).

using for GaAs the values $V_0 = 11.76$ meV and $\gamma = 27$ eV Å^3 without any adjustable parameter. We remark that these results are quite sensitive to the value of γ. Taking the smaller values suggested in some of the literature [1,27] results in larger relaxation times. The identification of the Dresselhaus coupling as the dominant channel for spin relaxation close to the MIT provides a strong motivation to pursue experimental and theoretical work in order to determine the precise value of γ.

Recently, spin-relaxation measurements have been performed in bulk CdTe at various doping densities [12]. A nonmonotonic behavior was obtained with an optimal value of $\tau_s = 2.5$ ns close to the MIT. The experimental data for densities near the MIT (∗ in Fig. 2) are well described by the numerically extracted values of τ_s (plus symbols) and by the prediction of Eq. (18) (red online dashed line). We remark that the numerical calculations are universal and that the material parameters enter upon performing the scaling procedure. The agreement between the theory and experiment for both GaAs and CdTe in spite of their dissimilar material parameters illustrates the wide applicability of our results. In narrow-gap semiconductors, like InAs and InSb, the particularly large Bohr radii lead to very long Dresselhaus relaxation times, which in the first case are even longer than those yielded by the extrinsic coupling [19]. However, the extremely low critical densities of these materials make it difficult to probe the physics of spin relaxation in the impurity band. Consequently, the low-density spin relaxation is proposed to be governed by other mechanisms [8].

In conclusion, we have identified a spin-relaxation mechanism characteristic of electrons on the metallic side of the metal-insulator transition in the impurity band of semiconductors, thereby solving a long-standing problem in spintronics. Our mechanism is derived from the Dresselhaus spin-orbit coupling. It dominates over the usually stronger extrinsic counterpart in the landscape of hydrogenic impurities in semiconductors with zinc blende structure and provides relaxation times that are in good agreement with the experimentally measured values.

We gratefully acknowledge support from the ANR through Grant No. ANR-08-BLAN-0030-02, the Collège Doctoral Européen of Strasbourg, UBACYT (Grant No. X495), ANPCYT (Grant No. PICT 2006-02134), program ECOS-Sud (action A10E06), and the ITN European Project NanoCTM (Grant No. 234970).

[1] J. Fabian *et al.*, Acta Phys. Slovaca **57**, 565 (2007).
[2] M. W. Wu, J. H. Jiang, and M. Q. Weng, Phys. Rep. **493**, 61 (2010).
[3] R. J. Elliot, Phys. Rev. **96**, 266 (1954).
[4] Y. Yafet, in *Solid State Physics*, edited by F. Seitz and D. Turnbull (Academic, New York, 1963), Vol. 14, pp. 1–98.

[5] M. N. Alexander and D. F. Holcomb, Rev. Mod. Phys. **40**, 815 (1968).
[6] J. M. Kikkawa and D. D. Awschalom, Phys. Rev. Lett. **80**, 4313 (1998).
[7] M. Oestreich *et al.*, Phys. Rev. Lett. **95**, 216603 (2005).
[8] J.-N. Chazalviel, Phys. Rev. B **11**, 1555 (1975).
[9] V. Zarifis and T. G. Castner, Phys. Rev. B **36**, 6198 (1987).
[10] R. I. Dzhioev *et al.*, Phys. Rev. B **66**, 245204 (2002).
[11] M. Römer *et al.*, Phys. Rev. B **81**, 075216 (2010).
[12] D. Sprinzl *et al.*, Phys. Rev. B **82**, 153201 (2010).
[13] W. H. Lau, J. T. Olesberg, and M. E. Flatté, Phys. Rev. B **64**, 161301(R) (2001).
[14] J. H. Jiang and M. W. Wu, Phys. Rev. B **79**, 125206 (2009).
[15] B. I. Shklovskii, Phys. Rev. B **73**, 193201 (2006).
[16] K. V. Kavokin, Phys. Rev. B **64**, 075305 (2001).
[17] W. O. Putikka and R. Joynt, Phys. Rev. B **70**, 113201 (2004).
[18] I. S. Lyubinskiy, A. P. Dmitriev, and V. Yu. Kachorovskii, JETP Lett. **85**, 55 (2007).
[19] P. I. Tamborenea, D. Weinmann, and R. A. Jalabert, Phys. Rev. B **76**, 085209 (2007).
[20] P. Nozières and C. Lewiner, J. Phys. (Paris) **34**, 901 (1973).
[21] H.-A. Engel, E. I. Rashba, and B. I. Halperin, in *Handbook of Magnetism and Advanced Magnetic Materials*, Vol. 5, edited by H. Kronmüller and S. Parkin (Wiley, Chichester, 2007).
[22] *Spin-Orbit Coupling Effects in Two-Dimensional Electron and Hole Systems*, edited by R. Winkler (Springer-Verlag, Berlin, 2003).
[23] M. Cardona, N. E. Christensen, and G. Fasol, Phys. Rev. B **38**, 1806 (1988).
[24] A. N. Chantis, M. van Schilfgaarde, and T. Kotani, Phys. Rev. Lett. **96**, 086405 (2006).
[25] J. J. Krich and B. I. Halperin, Phys. Rev. Lett. **98**, 226802 (2007).
[26] V. A. Marushchak, M. N. Stepanova, and A. N. Titkov, Sov. Phys. Solid State **25**, 2035 (1983).
[27] B. Jusserand *et al.*, Phys. Rev. B **51**, 4707 (1995).
[28] W. Knap *et al.*, Phys. Rev. B **53**, 3912 (1996).
[29] L. Meier *et al.*, Nature Phys. **3**, 650 (2007).
[30] T. Matsubara and Y. Toyozawa, Prog. Theor. Phys. **26**, 739 (1961).
[31] G. A. Intronati *et al.*, arXiv:1102.4760.
[32] We have obtained excellent agreement between Eq. (13) and the numerically computed time evolution starting from an on-site state.
[33] G. A. Thomas *et al.*, Phys. Rev. B **23**, 5472 (1981).
[34] P. H. Roberts and H. D. Ursell, Phil. Trans. R. Soc. A **252**, 317 (1960).